Probing the Conformational Heterogeneity of the Acetylaminofluorene-Modified 2′-Deoxyguanosine and DNA by ^{19}F NMR Spectroscopy†

Bongsup P. Cho* and Li Zhou

Department of Biomedical Sciences, College of Pharmacy, University of Rhode Island, Kingston, Rhode Island 02881

Received January 26, 1999; Revised Manuscript Received April 8, 1999

ABSTRACT: ^{19}F NMR spectroscopy was used to probe the conformation of a DNA adduct derived from the carcinogen 7-fluoro-*N*-acetyl-2-aminofluorene (FAAF) in three structural contexts: as a monomer and incorporated into single- and double-stranded DNA. The ^{19}F NMR spectrum of dG-C8-FAAF [*N*-(deoxyguanosin-8-yl)-*N*-acetyl-7-fluoro-2-aminofluorene] in methanol at −30 °C exhibited four interconvertible signals in a 11:52:26:11 ratio. Dynamic NMR analysis indicated that the four torsional isomers arise from restricted rotation about the amide (γ) (14.4 kcal/mol) and the guanyl−nitrogen (α) bonds. The conformational heterogeneity persisted in a single strand FAAF-12-mer, d(CTTCTTG[FAAF]-ACCTC), whose ^{19}F NMR spectrum at 22 °C and pH 7.0 gave only two signals in a 40:60 ratio, instead of four. The two ^{19}F signals followed a two-site exchange with the rotation barrier of 14.7 kcal/mol about the amide (γ') bond. A similar conformational theme was observed in the FAAF-12-mer duplex, d(CTTCTTG[FAAF]ACCTC)·d(GAGGTCAAGAAG), which revealed two ^{19}F resonances in a 41:59 ratio at 22 °C and pH 7.0. According to solvent-induced isotope and magnetic anisotropy effects, the two duplex conformers adopt exclusively a base displacement structure, being different only in their relative acetyl group orientations, cis ($\gamma' \sim 180°$) or trans ($\gamma' \sim 0°$). Dynamic NMR data indicated that the two conformers do not exchange over a wide range of temperatures. This contrasts with the nonacetylated counterpart, which exhibits an equilibrium between the "B-type" and "stacked" conformers [Zhou, L., et al. (1997) *J. Am. Chem. Soc. 119,* 5384−5389]. The exclusive stacked nature of the AAF adducts may provide insight into why AAF adducts are more mutagenic and prone to repair than the nonacetylated AF adducts.

Most mutagens and/or carcinogens undergo an oxidative metabolic activation in vivo and subsequently bind to DNA (*1*−*3*). This covalent adduct formation is recognized as an important step in the initiation of multistage tumorigenesis. Arylamine and amide carcinogens are an important class of chemical carcinogens, some of which induce tumors in experimental animals and humans (*4*). *N*-2-Acetylaminofluorene (AAF)[1] is a prototype arylamine carcinogen, which has been studied extensively (*5, 6*). When AAF reacts with DNA in vivo, two C8-substituted dG adducts are formed as major products; one retains the acetyl group (dG-C8-AAF), and the other is the nonacetylated form (dG-C8-AF). While the mutational spectra of these carcinogens in bacteria are complex and system-dependent, the AAF adduct gives rise to mainly frameshift mutations and the AF adduct produces both point and frameshift mutations. The mutagenic properties of these adducts have been much less consistent in mammalian cells (*7*−*11*). It has been suggested that the mutagenic potentials of these adducts may be modified by the presence of accessory proteins operating during translational synthesis in mammalian cells (*11*).

Nuclear magnetic resonance (NMR) spectroscopy (*12, 13*) in conjunction with site-specific mutagenesis (*14*) has emerged as a powerful tool for probing the structure-function relationships in adduct-initiated carcinogenesis. Recent NMR structural studies (*15*−*18*) have shown that AF-modified DNA duplexes adopt two slowly interconvertible conformations that are distinct in structure, namely, an undisturbed "B-type" (or external) conformer and a "stacked" conformer. The stacked conformer exhibits features of base displacement, in which the carcinogen is intercalated into the helix with the modified dG with either syn (*17*) or anti (*16*) glycosidyl alignment. O'Handley et al. (*19*) have investigated an AAF-modified 9-mer duplex and found evidence for conformational heterogeneities as well. The major conformer, which accounted for more than 70% of the total population, displayed the characteristics of the stacked conformer with a syn alignment of the modified dG. Intercalation structures similar to the stacked conformer have

† This work was supported in part by a grant from the American Cancer Society (CN-130).

* Corresponding author. Telephone: (401) 874-5024. Fax: (401) 874-5048. E-mail: bcho@uri.edu.

[1] Abbreviations: AAFF, *N*-acetoxy-*N*-2-(acetylamino)-7-fluorofluorene; ABP, 4-aminobiphenyl; AF, 2-aminofluorene; AAF, *N*-acetyl-2-aminofluorene; AP, 1-aminopyrene; COSY, correlation spectroscopy; dG, 2′-deoxyguanosine; dG-C8-AF, *N*-(deoxyguanosin-8-yl)-2-aminofluorene; dG-C8-AAF, *N*-(deoxyguanosin-8-yl)-*N*-acetyl-2-aminofluorene; dG-C8-FAF, *N*-(deoxyguanosin-8-yl)-7-fluoro-2-aminofluorene; dG-C8-FAAF, *N*-(deoxyguanosin-8-yl)-*N*-acetyl-7-fluoro-2-aminofluorene; DNA, deoxyribonucleic acid; FABP, 4′-fluoro-4-aminobiphenyl; FAAF, 7-fluoro-*N*-acetyl-2-aminofluorene; FAF, 7-fluoro-2-aminofluorene; FID, free induction decay; NMR, nuclear magnetic resonance spectroscopy; NOESY, two-dimensional nuclear Overhauser enhancement correlation spectroscopy; 1D, one-dimensional; T_m, optical melting point; TOCSY, total correlation spectroscopy; 2D, two-dimensional; UV, ultraviolet.

10.1021/bi990182d CCC: $18.00
Published on Web 05/15/1999

also been observed with the AF modification at various single strand-double strand junctions or with duplexes containing AF- or AAF-modified dG positioned opposite deletion sites (*20*−*24*). A recent review by Patel et al. (*13*) describes these and several other intriguing structures associated with arylamine-modified DNA.

Arylamine-induced conformational heterogeneity in DNA is modulated by both the nature of the carcinogen and the base sequence context surrounding the adduct site (*13*). We have previously shown that a 4-aminobiphenyl (ABP)-modified 15-mer duplex exists predominantly (>90%) in the B-type conformer (*25*), whereas an AF duplex in the same sequence adopts approximately an equal population of the B-type and stacked conformers (*15*). Interestingly, an 11-mer DNA duplex modified with a highly planar 1-aminopyrene (AP) adopts exclusively the stacked conformer (*26*). The higher content of the stacked conformer in duplexes modified with the planar AF and AP is due to their efficient stacking ability as compared to that of the less planar ABP and may account for their high incidence of frameshift mutation (*27*). Mao et al. (*17*) have shown that an AF-modified 11-mer duplex, d(CCATC[AF]GCTACC)·d(GGTAGCGATGG), exists as a 30:70 mixture of the B-type and stacked conformers. This is contrasted with the results obtained with the same adduct in d(T[AF]GA)·d(TCA) (60:40 mixture) (*15*) and d(AG[AF]G)·d(CCT) (50:50 mixture) (*16*) sequence contexts (vide supra). The same group has described the structure (*18*) of three DNA duplexes each containing the [AF]dG adduct opposite dC at guanines of the *Nar*I *Escherichia coli* restriction enzyme sequence, d[CTC$G_1G_2CG_3$CCATC]·d[GATGGCGCCGAG], a mutational hot spot for this carcinogen (*28*−*30*). The mutagenic potential for frameshift mutation is known to be the highest at G_3, although the chemical reactivities of the three guanines are similar. In accord with this expectation, the relative population of the stacked conformer observed for the C[AF]-G_3C sequence context was found to be 50%, which was higher than that found in the other two sites (*18*).

A basic underlying principle in the structural biology of DNA adducts is that an adduct is responsible for a specific mutation and has a predominant relevant structure and conformation (*14*). However, many DNA adducts, including those derived from arylamine carcinogens, induce complex and multiple types of mutations. One plausible scenario, which has been addressed elegantly by Loechler (*1*), is that a DNA adduct in vivo exists in multiple conformations, where each may yield a different mutation. Due to the spectral complexities of ^{1}H NMR, however, most structural studies of carcinogen-DNA adducts have focused on the major conformations. Since mutation is an infrequent biological event, observed mutations may result from the replication of an adduct in a minor conformation. Moreover, as elaborated above, the adduct-induced conformational heterogeneity in DNA is modulated by both the nature of carcinogen structure and the neighboring base sequence (*12*, *13*). Therefore, we need new structure-activity correlation strategies, in which conformations can be grouped into certain basic structures; otherwise, it will be extremely difficult, if not impossible, to pinpoint exactly which conformation is responsible for the observed mutation.

We have recently introduced ^{19}F NMR spectroscopy as a unique, alternative approach for monitoring the multiple

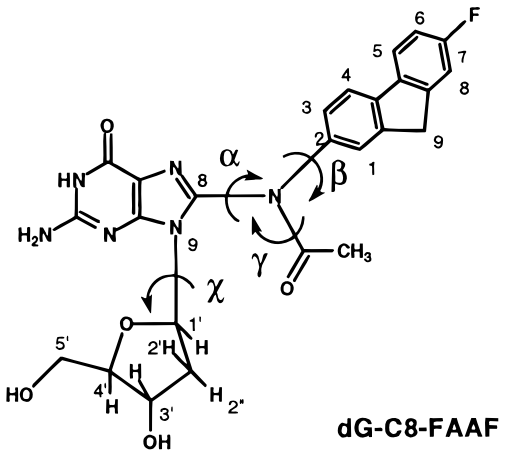

5′-C-T-T-C-T-T-G*-A-C-C-T-C-3′

Single Strand FAAF-12-mer (G* = dG-C8-FAAF)

5′-C-T-T-C-T-T-G*-A-C-C-T-C-3′
3′-G-A-A-G-A-A-C -T-G-G-A-G-5′

Double Strand FAAF-12-mer (Duplex) (G* = dG-C8-FAAF)

FIGURE 1: Chemical structures, numbering, and torsional angles of dG-C8-FAAF [*N*-(deoxyguanosin-8-yl)-*N*-2-(acetylamino)-7-fluorofluorene] and the base sequence of the single- and double-strand FAAF-modified 12-mer. The dihedral angles A−B−C−D are defined according to ref *58*: α, N9−C8−N−C2 (AAF); *β*, C8−N−C2−C1 (AAF); *γ*, C8−N−Cm−Cm; and *χ*, O4′−C1′−N9−C4. Cm and Cm represent the carbonyl and methyl carbons in the acetyl group, respectively. The angle A−B−C−D is measured by a clockwise rotation of D with respect to A, looking down the B−C bond. Corresponding torsion angles in the single- and double-strand FAAF-modified 12-mer DNA are designated as α′, *β*′, and *γ*′, respectively (see the text).

conformeric equilibria of DNA duplexes modified by fluorine-labeled AF and ABP (*31*). In this paper, we report the ^{19}F NMR probing of the conformational heterogeneity associated with the fluorine-labeled AAF adducts at three distinctive structural stages, i.e., monomeric and single- and double-stranded adducts (Figure 1). The unique static and dynamic ^{19}F NMR results obtained with these adducts will be discussed in terms of distinct mutagenic differences between the AF and AAF adducts.

EXPERIMENTAL PROCEDURES

Warning

2-Fluoro-7-nitrofluorene and their amino and amide derivatives are potential carcinogens, and therefore should be handled in a hood while wearing protective clothing.

Chemicals

2-Fluoro-7-nitrofluorene and 2′-deoxyguanosine (dG) were purchased from Aldrich Chemical Co. (Milwaukee, WI). Oligodeoxynucleotides [d(CTTCTTGACCTC) and d(GAG-

GTCAAGAAG)] were obtained from Biosource International-Keystone Laboratory (Camarillo, CA). HPLC grade solvents were obtained from Fisher Scientific, Inc. (Pittsburgh, PA). DNase I, phosphodiesterase I, and alkaline phosphatase were purchased from Sigma Chemical Co. (St. Louis, MO). All other reagent chemicals were obtained from Aldrich Chemical Co.

Instruments

High-resolution electron impact mass spectra (HRMS) were obtained on a Micromass 70-VSE instrument at the University of Illinois Mass Spectrometry Laboratory (Urbana, IL). Electrospray mass spectra of the monomeric dG-C8-FAAF adduct were recorded on a Micromass VG Quattro triple-quadrupole mass spectrometer at the Northeastern University Barnett Mass Spectrometry Laboratory (Boston, MA).

Samples were concentrated using a model AES 1000-120 SpeedVac concentrator (Forma Scientific, Inc., Marietta, OH). HPLC data were collected on a Waters Associates system equipped with model 501 pumps, a U6K injector, a 680 automated gradient controller, and a Hitachi L-3000 photodiode array detector. Separations were conducted using either a 5 μm Ultrasphere ODS analytical (4.6 mm $\times$ 250 mm) or semipreparative column (10.0 mm $\times$ 250 mm) from Beckman Instruments (San Ramon, CA). Optical melting points were measured on a Hitachi U-2000 spectrophotometer equipped with a model 9000 Isotemp refrigerated circulator (Fisher Scientific).

NMR Sample Preparation

The monomer dG-C8-FAAF adduct ($\sim$3 mg) was dissolved in methanol-d_4 and subjected to temperature-dependent ^{1}H and ^{19}F NMR experiments. The FAAF-modified 12-mer [d(CTTCTT[FAAF]GACCTC)] (75 $\times$ A_{260}) was dissolved in a pH 7.0 H_2O buffer containing 100 mM NaCl, 10 mM sodium phosphate, and 100 μM tetrasodium EDTA, and annealed with an equimolar complementary strand, d(GAG-GTCAAGAAG) (88 $\times$ A_{260}). The buffered sample required for analysis of the nonexchangeable protons was lyophilized three times from 99.96% D_2O and finally adjusted to 250 μL with 99.996% D_2O (designated as D_2O buffer). For imino proton spectra, the lyophilized sample was dissolved in 250 μL of 90% H_2O/10% D_2O (v/v) (designated as H_2O buffer). The NMR sample solutions were degassed with argon before capping.

NMR Experiments

^{1}H NMR spectra were obtained on a DPX400 Bruker NMR spectrometer, operating at 400 MHz. Chemical shifts are reported in parts per million downfield from internal tetramethylsilane (TMS) and 2,2-dimethyl-2-silapentane-5-sulfonate, sodium salt (DSS), for organic and aqueous samples, respectively. For observation of imino protons, one-dimensional (1D) proton spectra in H_2O buffer were collected with 16K data points over a 9980 Hz sweep width. The H_2O resonance was suppressed by using a 1-1 jump and return pulse sequence (*32*) with the carrier frequency set on the H_2O resonance. COSY experiments in D_2O buffer were acquired in the magnitude mode. A total of 256 t_1 increments was collected and processed by a 512 $\times$ 512 two-dimensional (2D) FT, and 16 scans were collected for each t_1 increment. The data were apodized with an unshifted sine-bell window function in both dimensions before Fourier transformation. TOCSY spectra were measured using a mixing time of 2.5 ms and a trim pulse of 30 μs. The time-proportional phase increment (TPPI) algorithm was used to obtain a phase sensitive mode. A total of 512 t_1 increments was collected and processed by a 2K $\times$ 1K 2D FT, and 48 scans were collected for each t_1 increment. Sixteen dummy scans were employed for each FID.

^{19}F NMR spectra were obtained on the same DPX400 NMR spectrometer, operating at 376.5 MHz and were referenced relative to the external $CFCl_3$. The available 5 mm probe did not allow proton decoupling. Two-dimensional ^{19}F NMR exchange experiments were carried out using a NOESY pulse sequence (*33*). Detailed NMR parameters are included in the figure legends.

Complete Line-Shape Analysis

Theoretical line shapes for two- or four-site exchange systems with different populations were generated by using a Windows program (WinDNMR: Dynamic NMR Spectra for Windows, version 1.5, *Journal of Chemical Education* Software Series D, Volume 3, Number 2; H. J. Reich, Department of Chemistry, University of Wisconsin, Madison, WI) and fitted with experimental spectra (*34*, *35*).

Optical Melting Experiments

The temperature-dependent absorption change for the FAAF-12-mer duplex at 260 nm was analyzed on a Hitachi U-2000 spectrophotometer equipped with a model 9000 Isotemp refrigerated circulator (Fisher Scientific, Inc., Pittsburgh, PA). The midpoint transition temperature (T_m) of the FAAF duplex obtained by the procedure of Marky and Breslauer (*36*) was 34 $\pm$ 1 °C for a duplex concentration of 5 μM.

Preparation of Adducts

N-Acetoxy-N-2-(acetylamino)-7-fluorofluorene (AAFF) is an activated amide ester carcinogen, which was prepared starting from 2-fluoro-7-nitrofluorene (Aldrich) by a modification of the procedure of Cramer et al. (*37*). 2-Fluoro-7-nitrofluorene (92 mg, 0.4 mmol) was dissolved in a mixture of acetic anhydride (0.4 mL), ethyl acetate (4 mL), pyridine (4 mL), and 10% Pd/C (14 mg). The mixture was then hydrogenated under an atmospheric pressure. After being stirred for 4 h at room temperature, the mixture was filtered through Celite, and evaporated under reduced pressure. The dark-colored concentrate was poured onto ice water with vigorous shaking. The resulting yellow precipitate was filtered and dried. The solid was sufficiently pure (>97% by HPLC) to be used for the next step without further purification: HPLC (90% methanol/10% H_2O, isocratic, 1 mL/min) t_R 3.24 min; ^{1}H NMR ($CDCl_3$) δ 7.75 (m, 2*H*, H4,5), 7.64 (s, 1*H*, H1), 7.47 (d, 1*H*, H3, $J_{3,4}$ = 7.9 Hz), 7.26 (d, 1*H*, H8, $J_{8,F}$ = 7.9 Hz), 7.11 (dd, 1*H*, H6, $J_{5,6}$ = 8.3 Hz, $J_{6,F}$ = 8.3 Hz), 3.92 (s, 2*H*, H9), 2.22 (s, 3*H*, $COCH_3$), 2.09 (bs, 3*H*, $OCOCH_3$); UV λ_{max} 273, 302 nm (shoulder); LRMS *m*/*z* (relative intensity) 299 (M^+, 33%), 257 ([M^+ $-$ CH_2CO], 40%), 241 ([M^+ $-$ CH_3CO_2], 39%), 215 ([M^+ $-$

Table 1: ^{1}H NMR Chemical Shifts in Parts per Million of dG-C8-FAAF at 35 and −30 °C[a,b]

		−30 °C			
assignment	35 °C	conformer I	conformer II	conformer III	conformer IV
F1[c]	7.68 (br)		∼7.78 (br)		
F3	7.48 (br)		∼7.60 (br)		
F4	7.80−7.83		7.80−7.90		
F5	7.80−7.83		7.80−7.90		
F6	7.10	7.15	7.18	7.09	7.15
F8	7.30	7.37	7.30	7.44	7.37
F14	3.94	3.97	3.97	3.97	3.97
G1′	6.27	6.33	6.26	6.39	6.33
G2′	3.01	3.14	2.84	2.84	3.14
G2″	2.23	2.28	1.52	2.03	2.07
G3′	4.57	4.64	4.45	4.57	4.61
G4′	4.05	4.13	4.04	4.09	4.13
G5′,5″	3.75−3.88		3.71−3.95		
CH_3	2.17	2.18	2.22	2.11	2.19

[a] Assigned by COSY and TOCSY experiments. [b] Recorded in methanol-d_4. [c] F represents fluorene and G dG.

$2CH_2CO$], 100%), 197 ($FArN^+$, 73%), 183 (Ar^+, 14%), 170 (36%); HRMS calcd for $C_{17}H_{14}NO_3F$ 299.0957, found 299.0958.

N-(Deoxyguanosin-8-yl)-N-2-(acetylamino)-7-fluorofluorene (dG-C8-FAAF). The monomer dG adduct was prepared by following a general literature method (*38*), except that the adduct was isolated by filtration. *N*-Acetoxy-*N*-2-(acetylamino)-7-fluorofluorene (AAFF, 35 mg) in 10 mL of absolute ethanol was added dropwise to a pH 7.0 citrate buffer (10 mM) solution containing 10 mg of dG. The mixture was stirred at 37 °C under an argon atmosphere. After 8 h, a second batch of AAFF (20 mg) was added to the mixture. On-line HPLC analysis indicated that the reaction was >90% complete after the mixture had been stirred for 24 h. The mixture was evaporated to dryness under reduced pressure and the residue partitioned between ether and water. This resulted in precipitation of a brown solid, which was collected by filtration and found to contain exclusively the monomer product. HPLC analysis indicated that the aqueous layer contains mainly the unreacted dG, while the ether layer consists primarily of decomposition products of AAFF. Pure dG-C8-FAAF was obtained by repeated purification using semipreparative reverse phase HPLC (20 min linear gradient, from 60 to 90% methanol in H_2O, at a rate of 2 mL/min). The yield was in the range of 30−50% based on the starting dG: HPLC t_R 13.71 min; UV λ_{max} 278, 305 nm (shoulder); ^{1}H NMR, see Table 1; ^{19}F NMR (methanol-d_4 at −30 °C) δ −116.8, 116.9, −117.3, −117.5 (see Results for details); electrospray MS (30 eV) *m*/*z* 507 ([M + H]), 391 ([M + H − dG]); MS (70 eV) *m*/*z* 349 ([M + H − dG − CH_2O]), 332, 183, 171.

FAAF-Modified 12-mer. The FAAF-modified 12-mer was prepared similarly by treating d(CTTCTTGACCTC) with AAFF at 37 °C (*31*). Twenty milligrams of AAFF in 3 mL of absolute ethanol was added dropwise to 10 mL of a 10 mM citrate buffer solution (pH 7.0) containing the 12-mer oligodeoxynucleotide. After the mixture had been stirred for 8 h under a nitrogen atmosphere, the excess ethanol was evaporated and the aqueous layer extracted several times with ether. The aqueous layer, which contained the adduct, was concentrated and purified by semipreparative HPLC (30 min linear gradient, from 5 to 25% acetonitrile in 10 mM ammonium acetate, at a rate of 2 mL/min). The yield which was >98% pure was approximately 40%: HPLC t_R 20.34 min; UV λ_{max} 268, 305 nm (shoulder). The modified oligodeoxynucleotide was characterized by a standard three-step enzymatic degradation analysis (*31*, *39*, *40*). The presence of a single dG-C8-FAAF adduct in the enzymatic hydrolysate mixture was confirmed by comparison of the HPLC retention time and UV spectral pattern with those of a standard (see Results for further NMR characterization of the FAAF-12-mer).

RESULTS

Preparation of the Model Adducts. The model ^{19}F NMR probes chosen for this study are *N*-(deoxyguanosin-8-yl)-*N*-2-(acetylamino)-7-fluorofluorene (dG-C8-FAAF) and a 12-mer oligodeoxynucleotide containing a single dG-C8-FAAF. The structure of dG-C8-FAAF along with the numbering system, torsional angles, and the DNA base sequence are shown in Figure 1. The main rationale for choosing this carcinogen was because fluorine substitution at the longest axis (i.e., 7-position) does not alter the carcinogenicity (*41*−*43*) or the metabolic and conformational profiles of the parent non-fluoro compound (AAF) (*44*, *45*). The 12-mer base sequence employed in this study is essentially that of the 15-mer mouse ras sequence [d(TACTCTTCTTGACCT)·d(AGGTCAAGAAGAGTA)] used in our earlier ^{1}H NMR studies (*15*), but shortened to improve synthesis and spectral interpretation without perturbing the unique conformational features at the adduct site. The 12-mer sequence was used in our previous ^{19}F NMR work on the nonacetylated FAF- and FABP-modified adducts (*31*).

Synthesis of the adducts was accomplished by treatment of dG or d(CTTCTTGACCTC) with *N*-acetoxy-*N*-2-(acetylamino)-7-fluorofluorene (AAFF). The latter is an activated form of the model carcinogen, which was prepared by a partial hydrogenation of 2-fluoro-7-nitrofluorene in the presence of acetic anhydride and pyridine. The identity of the *N*-acetyl-*N*-acyloxyl structure in AAFF was confirmed by mass and NMR spectral data. The mass fragmentation pattern is similar to that of the non-fluoro analogue (*46*) in that the molecular ion at *m*/*z* 299 expelled the acetyl (257, $M^+ - CH_2CO$) and the acyloxyl (241, $M^+ - CH_2COO$) radicals separately, as well as two acetyl radicals simultaneously affording the base ion at *m*/*z* 215. In the ^{1}H NMR spectrum, the 2.09 ppm resonance belonging to the *N*-acetyl protons was significantly broadened compared to that of the

O-acyloxyl at 2.22 ppm, further substantiating the presence of an amide-ester functionality (*47*, *48*).

The structure of dG-C8-FAAF was fully characterized by means of UV, mass, and NMR spectral data. Its UV absorption pattern is similar to that of the non-fluoro analogue, dG-C8-AAF (*39*), but differs significantly from the nonacetylated dG-C8-FAF (*31*). The identity of dG-C8-FAAF was further confirmed by electrospray mass spectrometry. The mass fragmentation resembles closely that of dG-C8-FAF (*31*), except for the presence of an acetyl group. The electrospray spectrum at 30 eV exhibited $[M + H]^+$ at *m*/*z* 507 and a fragment ion at *m*/*z* 391, which is consistent with the loss of the dG moiety. The presence of *m*/*z* 349 fragmentation at 70 eV supports the presence of the acetyl group ($[M + H - dG - CH_2O]$). The ^{1}H NMR spectrum of dG-C8-FAAF at the probe temperature (22 °C) exhibited a mixture of broad and narrow resonances, indicating multiple conformations (Figure A in the Supporting Information). This is contrasted with the nonacetylated dG-C8-FAF, which revealed only narrow proton signals under the same condition (*31*). Upon lowering of the temperature to −30 °C, the monomer displayed four distinct subspectra.

The FAAF-modified 12-mer was purified and characterized similarly as described for the FAF analogue (*31*). The UV spectrum of the FAAF-12-mer exhibited a shoulder around 300 nm (not shown), which is characteristic of the extended conjugation expected from an oligodeoxynucleotide containing AAF rather than AF (*39*, *49*, *50*). The presence of an acetamido functionality in the adduct is evidenced by its pronounced temperature-sensitive line broadening in the ^{1}H NMR spectra (see below) (*48*). The existence of a single adduct, dG-C8-FAAF, in an enzymatic hydrolysate of the modified DNA was confirmed by comparison of its on-line HPLC and UV characteristics with those of a standard (*31*).

Four Torsional Conformers of dG-C8-FAAF. The 400 MHz ^{1}H NMR spectrum at 22 °C exhibited a mixture of narrow and broad signals, indicating the occurrence of multiple conformations (Figure A in the Supporting Information). The line broadening was notable especially with the sugar H2′, H2″, and H3′ protons, as well as with the aminofluorene H1 and H3 protons that are adjacent to the acetamido group. At 35 °C, the aromatic protons were somewhat narrowed, while the sugar H2″ proton signals became extremely broadened. All resonances were collectively broadened at 0 °C, but became narrowed substantially on further lowering the temperature to −30 °C, in which four clearly discernible subspectra were obtained. While the signals in the aromatic region were severely congested, the acetyl and the sugar H1′, H3′, and H4′ protons were relatively well-resolved (Figure 2). The intramolecular sugar proton connectivities (H1−H2′ and H2″−H3′−H4′) within each subspectrum were established by analyses of COSY and TOCSY experiments (not shown), and the results are summarized in Table 1. The relative populations occurred in a 23:11:57:9 ratio, as measured for the four well-separated acetyl proton signals at 2.22, 2.19, 2.18, and 2.10 ppm, respectively (Figure 2c).

These results indicate that dG-C8-FAAF adopts four interconverting conformers through chemical exchange and are reminiscent of an earlier NMR study with the corresponding nonfluorinated 5′-monophosphate analogue (dGMP-C8-AAF). Using temperature-dependent ^{1}H and ^{13}C NMR

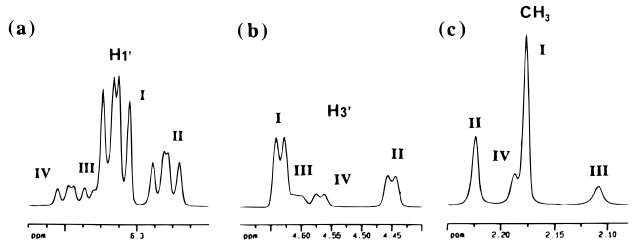

FIGURE 2: Expanded portions [(a) H1′ (6.36−6.26 ppm), (b) H3′ (4.70−4.40 ppm), and (c) $COCH_3$ (2.25−2.05 ppm)] of the ^{1}H NMR spectrum of dG-C8-FAAF recorded in methanol-d_4 at −30 °C. The data were apodized with a Lorentzian to Gausssian resolution enhancement window function using a line broadening of −1 Hz and the GB factor of 0.12. The conformeric assignments (I−IV) were made according to the structure shown in Figure 3 (see the text).

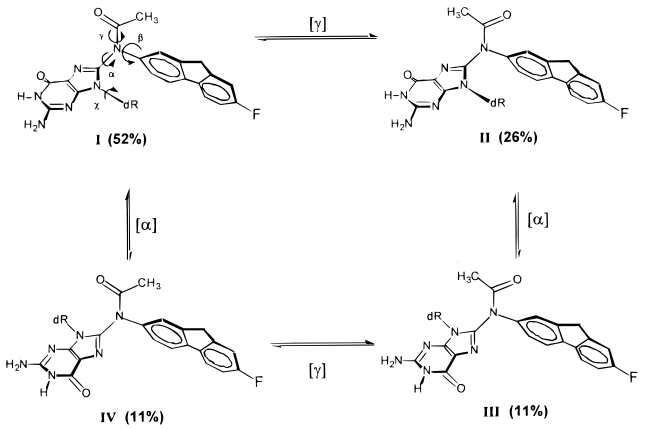

FIGURE 3: Schematic representation of the cyclic interconversion between the four conformers (I, II, III, and IV) of dG-C8-FAAF. The torsion angle values of α and γ shown here were taken from ref *51*: I, 90° and 180°; II, 270° and 0°; III, 90° and 0°; and IV, 270° and 180°. The torsion angle β was kept at 60° for all four conformers. See Figure 1 for the definition of torsion angles. The relative percent population based on ^{19}F NMR measurement at −30 °C is shown (see the text).

spectroscopy, Evans et al. (*51*) showed that dGMP-C8-AAF exists in four interchangeable torsional isomers owing to large rotation barriers about the amide (γ) and guanyl−nitrogen (α) bonds (Figure 1). Their principal reasoning for the restriction about the γ bond was based on the unusual shielding of the protons and carbons ortho to the acetamido moiety and their close resemblance to those observed with the cis and trans isomers of *N*-acetoxy-*N*-acetyl-2-aminofluorene (*N*-AcO-AAF) (*48*). On the other hand, large differences in the chemical shifts of the H2′ and H2″ sugar protons among the isomers were attributed to the restricted rotation about the guanyl−nitrogen bond (α). The relative populations of dGMP-C8-AAF according to decreasing intensities were 53:26:13:8, which were assigned respectively to conformer I ($\gamma = 180°$ and $\alpha = 90°$), conformer II ($\gamma = 180°$ and $\alpha = 270°$), conformer III ($\gamma = 0°$ and $\alpha = 0°$), and conformer IV ($\gamma = 0°$ and $\alpha = 90°$) (see Figure 3) (*51*). The striking similarities in the ^{1}H NMR subspectral patterns and relative population ratios suggest that the two adducts, dGMP-C8-AAF and dG-C8-FAAF, maintain a similar sets of conformers; hence, the four conformers of dG-C8-FAAF have been assigned accordingly: 57% conformer I, 23% conformer II, 11% conformer IV, and 9% conformer III (Figure 3).

Despite the similarity in their overall ^{1}H subspectral patterns, there are some notable differences. In general, deshielding of the H2′ resonance relative to that of dG is considered a good indicator for increased population of the syn conformation (*52*). The close proximity of the H2′ sugar proton to the guanine N3 in the syn conformation is believed to be responsible for the downfield shift. Compared to those of dG, the H2′ resonances of dG-C8-FAAF at −30 °C were generally shifted to downfield; however, the magnitude (0.15−0.45 ppm) of the deshielding was significantly smaller than that (0.63−0.89 ppm) observed for the 5′-monophosphate analogue, dGMP-C8-AAF (see Table 1) (*51*). This result suggests that dG-C8-FAAF may adopt less of the syn conformation as compared to dGMP-C8-AAF. This is unexpected since the free 5′-hydroxyl group in dG-C8-FAAF may favor hydrogen bonding with the guanine N3, possibly shifting the equilibrium toward the syn domain. The occurrence of a similar intramolecular hydrogen bonding has been detected in certain methylated aniline nucleoside adducts (*53*). Such a possibility, however, does not exist in dGMP-C8-AAF. The H2′ resonances of dGMP-C8-AAF have been reported to be sensitive to temperature change (*51*). However, aside from line broadening due to exchange, there was little detectable temperature dependence in the H2′ resonances of dG-C8-FAAF.

Dynamic ^{19}F NMR Experiments. The ^{19}F NMR spectrum of C8-dG-FAAF recorded at −30 °C exhibited four well-separated signals at −116.8, −166.9, −117.3, and −117.5 ppm (Figure 4). The spectral pattern did not change on further lowering temperature to −50 °C. Their relative populations at −30 °C were 11, 52, 26, and 11%, respectively, which are slightly different but in relatively good agreement with those obtained with the ^{1}H NMR subspectra discussed above. It should be noted that the corresponding nonacetylated dG-C8-FAF has exhibited a single ^{19}F NMR resonance at −120.0 ppm under similar measuring conditions (*31*). The signals at −166.9 and −117.3 ppm can readily be assigned to conformers I and II (Figure 4), respectively, on the basis of the comparison of their population with that obtained with ^{1}H NMR, i.e., conformer I (52% ^{19}F and 57% ^{1}H) and conformer II (26% ^{19}F and 23% ^{1}H). Identification of the remaining two minor conformers, which exist in equal proportions (11%), was made on the basis of the analyses of dynamic ^{19}F NMR data (Figure 4). Briefly, the signal at −116.9 ppm, which was assigned to the conformer I, forms a two-site exchange pair with that at −116.8 ppm. Conformer II at −117.3 ppm exhibits a similar conformeric relationship with the most upfield signal at −117.5 ppm. These conformeric pair patterns presumably arise from torsional isomerism along with the guanyl−nitrogen bond (α) with a fixed amide bond configuration (Figure 3). Hence, the minor signals at −116.8 and −117.5 ppm have been assigned to conformers IV and III, respectively.

The interconversion nature of the four conformers of dG-C8-FAAF was established by two-dimensional ^{19}F NMR exchange experiments. Figure 5 shows the contour plots of the results recorded at three different temperatures, where off-diagonal peaks represent a magnetization transfer among the conformers. Even at −30 °C, all four conformers were rapidly interconverting, although the exchange between minor conformers III and IV was relatively slow. As the temperature was raised, rates of exchange increase dramatically between conformers IV and I, and between conformers II and III, in a pairwise fashion.

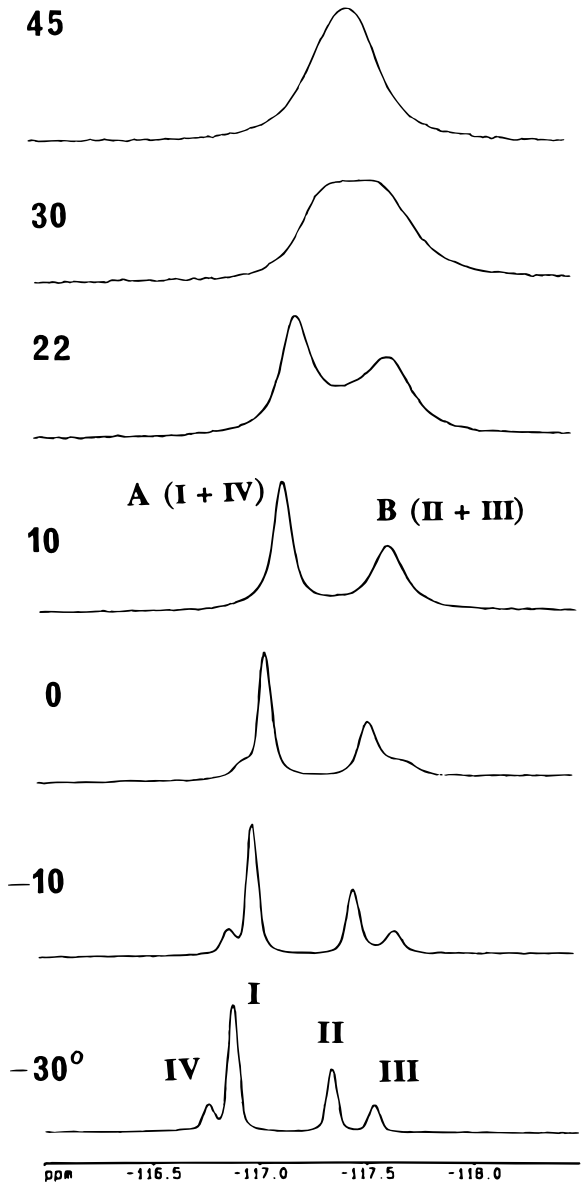

FIGURE 4: Temperature-dependent one-dimensional ^{19}F NMR spectra of dG-C8-FAAF recorded in methanol-d_4 for the region from −116.0 to −118.5 ppm. Before Fourier transformation, all data were apodized with an exponential window function using a line broadening of 5 Hz. The conformeric assignments (I−IV) were made according to the structure shown in Figure 3 (see the text).

The dynamic behavior of the four conformers of dG-C8-FAAF was investigated by analyses of one-dimensional ^{19}F NMR spectra recorded between −30 and 45 °C. The results, which are shown in Figure 4, represent a four-site chemical exchange process. As discussed above, these signals have been assigned to conformers IV, I, II, and III from the downfield to the upfield, respectively. While the four resonances were in relatively slow exchange at −30 °C, the exchange broadening took place in a pairwise fashion as the temperature was raised, giving rise to two time-averaged coalescent signals at 10 °C, A (−117.1 ppm, i.e., conformers IV and I) and B (−117.6 ppm, i.e., conformers II and III) in a 54:46 ratio. They eventually coalesced into a single broad resonance (−117.5 ppm) at 30 °C with line-shape changes

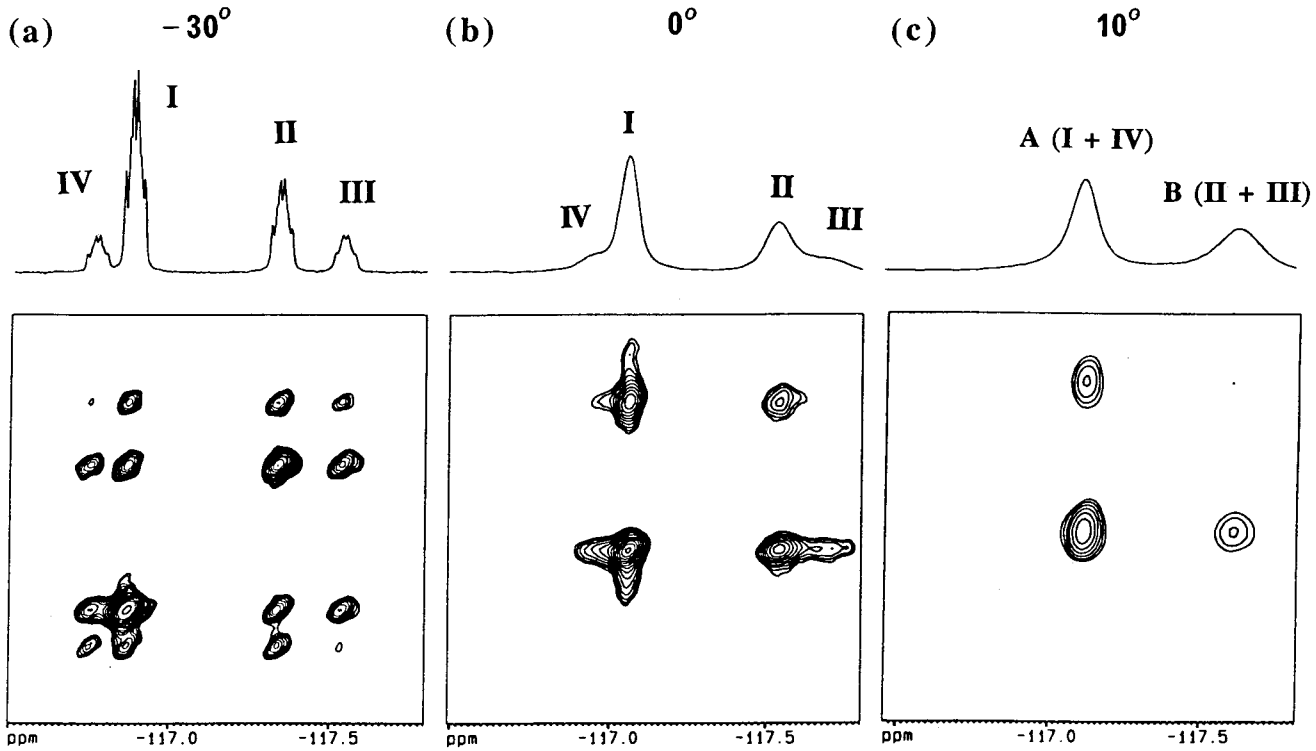

FIGURE 5: Two-dimensional ^{19}F NMR exchange spectra of dG-C8-FAAF recorded in methanol-d_4 at (a) −30, (b) 0, and (c) 10 °C for the region from −116.6 to −117.8 ppm. See Figure 3 for the structure of confomers I−IV. The spectra were obtained using a NOESY sequence (*33*). The time-proportional phase increment (TPPI) algorithm was used to obtain a phase-sensitive mode: sweep width of 2259 Hz, 1024 complex data points in t_2, 256 complex free induction decays in t_1, 72 scans, 16 dummy scans, recycle delay of 1.0 s, and mixing time of 700 ms. The data were subjected to exponential line broadening of 8 Hz in both dimensions and then zero-filled before Fourier transformation of the 1K × 512 data matrix. The data were not symmetrized.

characteristic of two-site exchange (*34*, *35*). On the temperature being raised further, the coalesced signal became sharper, and narrowed at 45 °C (−117.5 ppm). At this temperature, the rotations about the guanyl−nitrogen (α) and amide (γ) bonds are faster than the NMR scale. During the first coalescent period (−30 to 10 °C), rates of exchange between A (IV and I) and B (II and III) (for example, k_{IV-II}, k_{IV-III}, k_{I-II}, and k_{I-III}) appear to be very low. Therefore, the coalescent exchange between conformations IV and I and between conformations II and III can be regarded as two separate two-site exchange processes.

While there are many possibilities for a given system of the four ^{19}F signals, it can be best described by a semicyclic conformational interconversion similar to that previously proposed for dGMP-C8-AAF (Figure 3) (*51*). The rotation about the acetamido bond (γ) at 10 °C was sufficiently restricted, resulting in two principal conformers A and B at −117.12 and −117.61 ppm, respectively (Figure 4). This argument is supported by large temperature-dependent shielding of the aminofluorene H1 and H3 protons (ortho to the acetamido group) and by their unusual line broadening effect (vide supra). The presence of two additional conformers below 10 °C is a consequence of slowing of the rotation of bulky dG group about the fluorenyl−nitrogen bond (α). As in the case of the dGMP-C8-AAF work (*51*), the rotation about the fluorenyl−nitrogen (β) bond was assumed to be faster than the NMR scale. According to complete line-shape analysis in terms of a two-site exchange (*34*, *35*), the energy barrier to rotation about the γ bond, which is attributed for the presence of the first two set of conformers (A and B, Figure 4), was found to be 14.4 kcal/mol.

Single-Strand FAAF-12-mer. (1) ^1H NMR. The ^1H NMR spectrum of the single-strand FAAF-12-mer adduct in D_2O buffer taken at 22 °C exhibited an array of broad signals as a result of chemical exchange (Figure B of the Supporting Information). Partial resonance assignments have been made by comparisons with proton assignments for the monomeric dG-C8-FAAF adduct, and the unmodified 12-mer, as well as by the observation of the temperature dependence of resonances. Although the spectral quality was improved upon the temperature being raised to 40 °C, the broadening persisted particularly with the acetyl (2.18 ppm) and the fluorene H1 and H3 protons (7.3 and 7.5 ppm, respectively) that are located adjacent to the acetamido group. The observed line broadening is due to conformational heterogeneity and must be induced by the presence of a bulky acetyl group on the central nitrogen, since the same 12-mer sequence containing the nonacetyl FAF analogue exhibited no such unusual broadening.

The appearance of the aminofluorene protons in a relatively upfield region (6.6−7.4 ppm) is regarded as an indication of stacking interaction with adjacent bases. Similar collective shielding of aromatic protons was observed with several other AAF-modified single-strand DNAs (*50*). It has been shown that significant stacking occurs even as short as dimer (CG*) (*54*) and tetramer (TG*CA) (*55*), in which G* is modified by AAF and ABP (4-aminobiphenyl), respectively.

(2) ^{19}F NMR. In accord with the ^1H NMR data, the single-strand FAAF-12-mer in the ^{19}F NMR spectrum at 22 °C displayed two broad resonances at −115.1 and −115.3 ppm in a ratio of 2:3 (not shown). While the two signals were

significantly broadened at 5 °C, they coalesced into a single resonance at −115.1 ppm at 40 °C by following a typical pattern of two-site chemical exchange. Line-shape analyses (*34*, *35*) of the dynamic [19]F NMR data provided an interconversion energy barrier of 14.7 kcal/mol. This contrasts with the nonacetylated FAF analogue, which exhibited a single narrow [19]F resonance under identical experimental conditions (*31*).

Shapiro et al. (*56*) have examined the conformation of AAF-modified dG with all possible nearest neighbors and found that the principal effect of the acetyl group on the central nitrogen is the destabilization of anti conformations for the modified guanine. The bulky acetyl group induces the guanine base to adopt a syn conformation, resulting in a strong stacking interaction of the fluorene moiety with neighboring bases. Evans and Levine (*51*) have observed two proton subspectra for the dimeric AAF adduct (dCG[AAF]) in a ratio of 4:1, which have been assigned to conformers I ($\gamma' \sim 180°$)[2] and III ($\gamma' \sim 0°$) in the fully stacked state ($\alpha' \sim 90°$). The assignment was accomplished by analyzing the [1]H NMR spectra measured as a function of varying methanol concentration and temperature. Their results (*54*) are in good agreement with the calculations done by Shapiro et al. (*56*), except that the $\gamma' \sim 0°$ conformer (i.e., conformer III) was found to have the lowest energy.

Our NMR data, together with previous findings discussed above, indicate that the single-strand FAAF-12-mer exists in a 40:60 mixture of two slowly exchanging conformers at room temperature. The restricted rotations about the guanyl−nitrogen (α') and glycosyl (χ) bonds afford only two conformeric possibilities along the amide (γ') bond, instead of four as detected in the monomeric dG-C8-FAAF adduct (vide supra). The orientation of the acetyl group is defined as cis ($\gamma' \sim 180°$) or trans ($\gamma' \sim 0°$) depending on whether the carbonyl oxygen is located on the same or opposite side of the modified guanine (*54*). The calculated 14.7 kcal/mol energy barrier is in good agreement with those observed with the monomeric dG-C8-FAAF (14.4 kcal/mol) (vide supra) and the dimeric dCG(AAF) (*54*) adducts (14.3 kcal/mol). We were, however, unable to assign the two [19]F signals in the spectrum of the single-strand FAAF-12-mer to the specific individual trans or cis conformers.

Double-Strand FAAF-12-mer (Duplex). (1) [1]H NMR. The [1]H NMR spectrum of the FAAF-12-mer duplex recorded in a D_2O buffer at 22 °C (not shown) displayed a mixture of narrow and broad resonances. Again, this is a clear indication of the presence of multiple conformations. The intercalated nature of the carcinogen moiety in the duplex is also evident from the appearance of unusually broad fluorene proton signals in the upfield region (6.3−7.1 ppm) (*15*−*19*, *26*). On the temperature being raised to 65 °C, all signals became narrowed, while the upfield aromatic resonances were moved downfield and merged with other aromatic nucleic acid protons in the region of 7−8 ppm. A similar collective shielding of carcinogenic protons has been observed for the DNA duplexes modified with AAF (*19*) and AP (*26*), in which the carcinogenic moieties intercalate between flanking Watson−Crick base pairs.

[2] The primed torsional angles (α', β', and γ') in the single- and double-strand DNA are distinguished from those used for nucleoside.

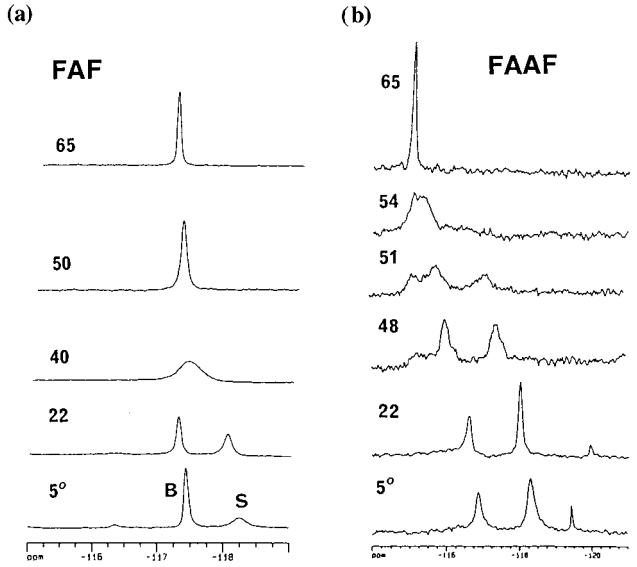

FIGURE 6: Temperature-dependent [19]F NMR spectra of the FAF- and FAAF-modified 12-mer duplexes recorded in H_2O buffer. The temperature range was 5−65 °C. Before Fourier transformation, all data were apodized with an exponential window function using a line broadening of 10 Hz.

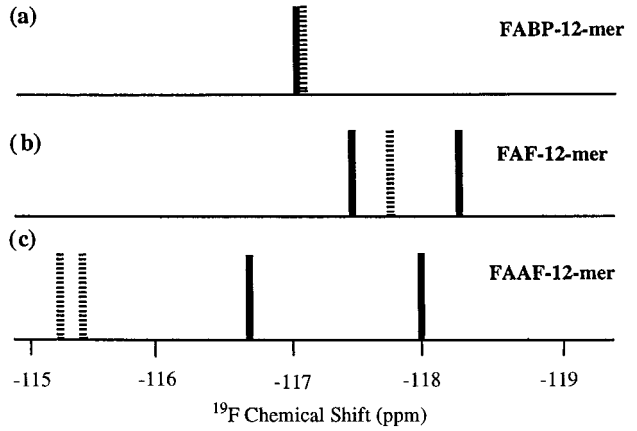

FIGURE 7: Schematic representation of [19]F NMR chemical shifts for the 12-mer oligodeoxynucleotides modified by the carcinogens FABP, FAF, and FAAF at the single- (dotted line) and double-strand (duplex) (solid line) levels.

The downfield region of the proton spectrum of the FAAF duplex recorded in a H_2O buffer at 18 °C is compared with those of the nonacetylated counterpart FAF and the control duplexes (Figure C of the Supporting Information). The varying intensities of the imino protons are similar to those of the FAF duplex, which was shown to adopt at least two conformers in slow exchange at this temperature (*31*). All the imino signals of the FAAF duplex were gradually broadened as the temperature increased and completely exchange broadened at around 42 °C.

(2) [19]F NMR. A [19]F NMR spectrum of the FAAF duplex at 22 °C exhibited two prominent signals at −116.7 and −118.0 ppm in a 41:59 ratio (Figure 6b). These chemical shifts represent a significant shielding from that of the single strand, and closely resemble those observed with the FABP and FAF duplexes (*31*).

Solvent-Induced Isotope Experiments. Figure 7 shows a schematic representation of the [19]F signals derived from the three fluorine-labeled FABP, FAF, and FAAF adducts in

both the single- and double-strand contexts. The FABP-12-mer duplex, which adopts exclusively the B-type conformer, exhibited a ^{19}F resonance at −116.9 ppm (Figure 7a, solid line) (*31*). The same adduct in a single-strand form (Figure 7a, dotted line) exhibited a resonance at a very similar chemical shift (−117.0 ppm). These results indicate that the FABP adduct in both the single- and double-strand DNA exists as the B-type conformer. The FAF duplex, on the other hand, exhibited two distinct ^{19}F signals at −117.4 and −118.3 ppm in a 55:45 mixture (Figure 7b), which have previously been assigned to the B-type conformer and stacked conformer, respectively (*31*). The conformer assignment was primarily based on solvent-induced isotope experiments (*57*−*59*). The expectation was that the exposed fluorine in the B-type conformer would be susceptible to large solvent effect, whereas the buried fluorine in the stacked conformer would not (*31*). The downfield (−117.4 ppm) B-type conformer signal was shifted upfield by 0.24 ppm, while the effect on the upfield (−118.3 ppm) stacked conformer signal was negligible (0.08 ppm). As anticipated, a comparable shielding (0.23 ppm) was observed for the sole signal in the spectrum of FABP duplex, which adopts predominantly the B-type conformer.

We have conducted similar isotope experiments to ascertain the nature of the two FAAF duplex conformers. The chemical shifts of the two signals changed very little (−0.04 ppm) when the deuterium content of the solvent increased from 10 to 100% at 18 °C. This lack of significant isotope effects contrasts with the results obtained with the corresponding nonacetylated FAF duplex discussed above. The result implies that both conformers of the FAAF duplex adopt a typical base displacement structure, in which the carcinogen moiety is intercalated into the helix, thus protecting the fluorine atoms on the fluorene moiety from exposure to solvent. This, coupled with strong syn preference for the C8-substituted guanine (vide supra), is in good accord with previous computational results, which have consistently predicted the syn conformation to be more stable than the anti for the AAF adduct at various sequence contexts (*56*).

The exclusive stacked conformation observed for the FAAF duplex is clearly due to the steric interference between the bulky acetyl group at the central nitrogen and the sugar phosphate backbone linked to the modified guanine. Thus, the syn guanine configuration limits the rotations about the guanyl (α') and fluorenyl−nitrogen (β') bonds, resulting in a cis−trans amide torsional isomerism depending on whether the carbonyl oxygen of the acetyl group is oriented the same as (for cis, $\gamma' \sim 180°$) or opposite from (for trans, $\gamma' \sim 0°$) the modified guanine residue. This is essentially an extension of a two-stage model that has been established with the FAAF adduct in both the monomeric (dG-C8-FAAF) and single-strand levels (vide supra).

The ^{19}F NMR chemical shift difference (1.3 ppm) observed between the cis and trans acetyl conformers of the FAAF duplex is relatively large compared to those with the monomeric (0.5 ppm) or single-strand AAF adducts (0.2 ppm). It may be due to a change in the geometry of the adduct. Although several bonds away, the orientation of the acetyl group at the central nitrogen has apparently a significant effect on the electron density of the fluorene ring. For example, it has been shown that the chemical shift differences for carbon resonances between the cis and trans isomers of *N*-acetoxy-*N*-acetyl-2-aminofluorene (*N*-AcO-AAF) and *N*-hydroxy-*N*-acetyl-2-aminofluorene (*N*-OH-AAF) were the largest for C1, C3, C11, and C14 (3−5 ppm) (*48*). The effect was observed throughout the whole ring system as evidenced by the significant upfield shift (0.7 ppm) of the remotely located C7, to which the fluorine label is attached (*51*).

Dynamic ^{19}F NMR Experiment. The FAAF-induced conformational heterogeneity at the duplex level was investigated by one- and two-dimensional dynamic NMR spectroscopy. Figure 6b shows a series of ^{19}F NMR spectra of the FAAF duplex measured as a function of different temperatures (5−65 °C). A temperature profile for the corresponding nonacetylated FAF duplex (*31*) is also shown for comparison (Figure 6a). The line widths of the two FAAF ^{19}F signals (Figure 6b) were not significantly altered until 40 °C, at which temperature the corresponding resonances of the FAF duplex completely coalesced (Figure 6a). The FAAF signals (Figure 6b) were broadened somewhat between 45 and 48 °C. Several additional resonances were formed on further raising the temperature to 51 °C. Although the signals were significantly broadened at 54 °C, giving rise to a single broad resonance, there were no truly identifiable coalescent signal(s) as observed in the case of the FAF duplex. Upon the temperature being raised further to 65 °C, the FAAF signals were merged to a narrow signal at −115.4 ppm, which represents a single average conformation of the unpartnered 12-mer adduct. It should be noted that the ^{19}F signals of the single-strand FAAF adduct resonate in the similar range (−115.0 to −115.3 ppm) (see Figure 7c, dotted lines).

The dynamic profiles of the FAAF duplex represent a simple helix−coil melting transition without any evidence of chemical exchange between the two major duplex conformers over a wide range of temperatures. Two-dimensional exchange experiments (not shown) conducted at various temperatures fail to provide any evidence of exchange between the two signals. The lack of dynamic exchange in the double-strand FAAF adduct is contrasted with a facile cis−trans amide bond torsional isomerism observed in the single-strand one, which followed a typical two-site exchange process with a rotation energy barrier of 14.7 kcal/mol (vide supra). It appears that the steric constraint between the bulky acetyl group and the nearby sugar and base atoms increases dramatically going from the single- to double-strand helixes.

The occurrence of several broad signals at 51 °C suggests the presence of multiple unstable intermediate conformations (Figure 6). Upon the temperature being raised, the double-helical structure unwound into individual coils, thereby relieving steric constraint on the central nitrogen at the adduct site. This lowers the energy barriers for the rotation of the guanyl (α') and fluorenyl−nitrogen (β') bonds as well as that of the amide (γ') bond, all of which could produce multiple conformations, thereby creating different ^{19}F nuclear environments. In this regard, it should be noted that the AF duplex adduct opposite a −1 deletion site exists in an equilibrium of the two conformers depending on whether the C9 edges of the fluorene ring face the major or minor groove at the intercalate site (*20*). The two β' rotamers were found to rapidly interconvert on the NMR time scale. The same authors have provided evidence for the existence of a similar rotameric interconversion of AF as well as the syn−

anti equilibrium for the AF adduct positioned opposite dC in a duplex (*17*).

The available data did not allow us to make assignments of the two ^{19}F signals into specific individual trans or cis conformers. It is worth noting though that the major conformer of an AAF-modified 9-mer duplex studied by O'Handley et al. (*19*) (vide supra) adopts a trans orientation ($\gamma' = 37°$), which exhibits an energy that is slightly lower than the corresponding cis one. Accordingly, the highly populated −118.0 ppm signal was tentatively assigned to that belonging to the trans isomer.

DISCUSSION

The ^{19}F NMR data presented in this paper convincingly demonstrate that the monomeric adduct dG-C8-FAAF exists in at least four different conformers in methanol at low temperatures (−30 to −50 °C). Since the nonacetylated counterpart dG-C8-FAF exhibits a single resonance under the same condition, it is clear that the presence of the bulky acetyl group places restrictions on the conformation at the central nitrogen. Temperature-dependent ^{19}F NMR studies showed that dG-C8-FAAF at 10 °C exists in an about 60:40 ratio of two energetically distinct conformations (A and B in Figure 4), which presumably arise from a large restricted rotation barrier (14.4 kcal/mol) about the amide bond (γ). Further lowering the temperature (−30 °C) resulted in two additional torsional conformers due to the restriction of the rotation along the guanyl−nitrogen (α) bond. The four torsional conformers interconvert rapidly over the wide range of temperatures that were utilized (Figure 5).

The same adduct (dG-C8-FAAF) embedded in a 12-mer single strand DNA, d(CTTCTTG[FAAF]ACCTC), revealed two slowly exchanging ^{19}F NMR signals in a 2:3 ratio. This result is contrasted with the nonacetylated counterpart FAF-12-mer, which exhibited a single narrow ^{19}F resonance under the identical experimental conditions (*31*). The observed conformational heterogeneity in the single-strand form is due to the presence of a bulky acetyl group at the central nitrogen. An extensive stacking of the fluorene moiety with the neighboring base is indicated by collective shielding of fluorene aromatic proton signals. The strong preference for the syn domain for the modified dG restricts the internal rotations on both the glycosyl (χ) and guanyl−nitrogen (α') bonds, resulting in only two conformeric possibilities about the amide bond [conformers I ($\gamma' \sim 180°$) and III ($\gamma' \sim 0°$], rather than four as detected for the monomeric adduct. The 14.7 kcal/mol energy barrier calculated for the restricted amide bond (γ') of the single strand adduct is also in good agreement with those observed for the monomeric dG-C8-FAAF (14.4 kcal/mol, this study) and dimeric (*54*) AAF adducts (14.3 kcal/mol). Theoretical calculations have shown that the energies of the two γ' conformers occur within a narrow range (2.1 kcal/mol), and the reversal of the acetyl group orientation has relatively little effect on the remainder of the overall single-strand structure (*56*).

A similar conformational heterogeneity persists in a double-strand duplex DNA, d(CTTCTTG[FAAF]ACCTC)•d(GAGGTCAAGAAG). The ^{19}F NMR spectrum revealed two ^{19}F NMR signals in a 41:59 mixture. While several conformational possibilities may exist at the duplex setting, two two-stage models based on the restricted rotations about the amide (γ') and glycosyl (χ) bonds can be envisioned. The γ' bond model is essentially an extension of that proposed for the single-strand FAAF adduct (vide supra). Thus, both conformers of the FAAF duplex adopt essentially the identical base displacement stacked structure, but differ only in their acetyl group orientation: trans ($\gamma' \sim 0$ °C) and cis ($\gamma' \sim 180$ °C) (Figure 3). Alternatively, the observed FAAF-induced conformational heterogeneity may arise from the restricted rotations about the glycosyl bond (χ) of the modified dG, e.g., anti and syn. Such a conformeric equilibrium has been observed with nonacetylated AF duplexes in several different base sequence contexts (*13*). The lack of a solvent-induced H−D isotope effect as well as the exclusive stacking of the carcinogenic moiety in the FAAF duplex clearly favors a cis−trans conformeric equilibrium over the B-type/stacked one. The steric interference between the bulky acetyl group at the central nitrogen and the sugar phosphate backbone is responsible for the preference of the syn guanine conformation.

The exclusive base displacement structure of the FAAF duplex deduced above is in good accord with those obtained with AAF adducts investigated in various sequence contexts (*19*, *23*, *24*). Using a combination of ^{1}H NMR, energy minimization, and molecular mechanics, O'Handley et al. (*19*) have shown that the AAF adduct positioned opposite dC in a 9-mer duplex exists in multiple conformations, with the major conformation being about 70% of the total. The modified dG in the major conformer adopts the syn conformation and resides in the major groove, while the fluorene moiety is inserted into the helix and protrudes into the minor groove. According to their NOESY-based energy-minimized structure, the torsion angles of the guanyl (α') and fluorenyl−nitrogen (β') bonds are 44° and 23°, respectively. The carbonyl oxygen of the acetyl group in the major groove was found to be trans ($\gamma' = 37°$) to the C8 position of the modified guanine. Milhe et al. (*23*, *24*) have reported the presence of multiple conformations for the AAF adduct positioned opposite a −1 as well as −2 deletion sites at the *Nar*I mutational hotspot of *E. coli*. Although interpretation of the NMR data was complicated due to chemical exchange, they all share the base displacement stacked structure as the major conformation. Conformational heterogeneity, thus, appears to be a common theme for the AAF adducts in DNA.

The AAF-induced conformational heterogeneity is not as clearly defined as that of the AF one, which was shown to adopt a well-characterized B-type−stacked equilibrium (*13*). In the work cited earlier, O'Handley et al. (*19*, *60*) made some efforts to define the structure of minor conformers of the AAF-modified 9-mer duplex. Of several theoretical models that have been mentioned, the torsional conformer with the cis acetyl group orientation (i.e., $\gamma' =$ near 180° domain) is of special interest in the context of our discussion. The cis conformer was calculated to have a slightly higher energy than the trans, which was the configuration adopted by the major conformer (vide supra). Shapiro et al. (*56*) have shown that the reversal of the acetyl orientation does not have much impact on the remainder of the overall single-strand DNA and that the energies of the two extremes occur within a narrow 2.1 kcal/mol range. A somewhat higher energy barrier difference (∼5.7 kcal/mol) was obtained for a misaligned slipped intermediate of the *Nar*I sequence, in

which the AAF-modified guanine and its 3′-neighbor cytosine in the template strand are unpartnered (*61*).

The exclusive stacking nature of the FAAF duplex conformers is similar to that observed with the AP-modified 11-mer duplex, in which the pyrene ring intercalates into the helix while the modified guanine is displaced into the major groove (*26*). The difference between the AP and AF adducts is presumably due to the much greater stacking ability between the aromatic amine ring and flanking base pairs of the larger pyrene ring compared to that of the smaller fluorenyl ring (*62*). However, the difference in the stacking ability between the AF and AAF adducts must be due to the bulky acetyl group present at the central nitrogen at the latter adduct site, which prohibits a facile syn−anti conformational interconversion.

Taken together, the available data support the presence of a cis−trans model for the FAAF-modified duplex. This is essentially an extension of a two-stage model that has been established with the FAAF adduct in both the monomeric (dG-C8-FAAF) and single-strand levels (vide supra). The lack of a discernible dynamic exchange between the two FAAF duplex conformers is probably due to the increased rotation energy barrier of the acetyl group located in the major groove at the duplex setting.

Biological Implications. Mutation takes place at single strand−double strand DNA junctions, known as replication forks, and involves a whole array of replication machinery, including a polymerase and other accessory proteins. It has been shown that an AF adduct exists in equilibrium between the B-type and stacked conformers and their interconversion occurs at a rate similar to that of the in vivo replication. A delicate balance in the equilibrium at the replication fork would probably be influenced by the base sequence contexts around the adduct site as well as the action of a polymerase and other proteins involved in replication. For example, the AF adduct at the primer−template junction adopts a stacked-type conformation, with the modified dG in syn alignment regardless of the presence of a normal partner dC, and a mismatched dA, or no partner opposite the adduct (*13*).

Our NMR data showed that an AAF adduct adopts exclusively the base displacement intercalated structure at both the single- and double-strand levels. The AAF-induced conformational heterogeneity arises solely from the difference in the orientation of the acetyl oxygen atom relative to the modified guanine. The mutagenic implication of the relative acetyl group orientation in a DNA setting is not known. However, the exclusive persistence of a stacked conformation at both single- and double-strand levels may be important since mutation takes place during replication, in which the adduct is exposed to a single strand−double strand junction or a bulge structure created by a slippage mechanism (*30*). The greater propensity of the AAF adducts to adopt the stacked conformer would allow the polymerase to pause longer at the lesion site. The longer the polymerase pauses at the replication fork, the better chance the adduct has to form a slippage intermediate, which eventually triggers −2 deletion mutation in a suitable base sequence, such as the *E. coli Nar*I hot spot (*30*). Recent theoretical calculations conducted by Roy et al. (*61*) indicate that the slipped mutagenic AAF intermediate is energetically more stable than its normally extended counterpart in the presence of AF and AAF in the syn modified dG. The exclusive adoption of the stacked conformation for the AAF adduct may explain why the AAF adduct is more prone to repair and mutation than the AF adduct.

Concluding Remarks. Our results demonstrate that the ^{19}F nucleus is extremely sensitive to conformational changes of the AAF-modified DNA adduct at various structural settings. Other nucleic acid isotopes such as ^{13}C, ^{15}N, or ^{31}P have previously been used to probe adduct structure, but shown to be much less sensitive and therefore not as practical (*12*, *13*, *48*, *51*, *63*). Although the detailed structural interpretation of ^{19}F NMR is rather limited, the sensitivity of ^{19}F NMR chemical shifts in the macromolecular environment and the lack of background noise (*58*, *59*) clearly offers advantages in dealing with adduct-induced multiple conformeric equilibria in vivo. An ultimate structural biology challenge in chemical carcinogenesis is to conduct adduct, site-specific mutagenesis in a conformationally specific manner (*1*) in a biologically simulated environment. This will require probing the adduct-induced conformational heterogeneity at the single strand−double strand junction in the presence of replication and repair enzymes, dNTPs, and divalent cations, all of which are important components for mutation. These experiments, which are otherwise difficult to conduct, should be feasible with the newly developed ^{19}F NMR approach.

ACKNOWLEDGMENT

We thank Dr. F. A. Beland for his critical reading of the manuscript and helpful comments. The electrospray mass spectrum of dG-C8-FAAF was generously provided by Dr. P. Vouros.

SUPPORTING INFORMATION AVAILABLE

Figures showing the temperature-dependent ^1H NMR spectra of the monomeric dG-C8-FAAF (Figure A) and the single-strand FAAF-modified 12-mer (Figure B) and imino proton spectra (Figure C) of the FAAF- and FAF-modified 12-mer and the unmodified 12-mer duplexes. This material is available free of charge via the Internet at http://pubs.acs.org.

REFERENCES

1. Loechler, E. L. (1996) *Carcinogenesis 17*, 895−902.
2. Dipple, A. (1995) *Carcinogenesis 16*, 437−441.
3. Hemminki, K., Dipple, A., Shuker, D. E. G., Kadlubar, F. F., Segerbäck, D., and Bartsch, H., Eds. (1994) *DNA Adducts: Identification and biological significance*, IARC Scientific Publications No. 125, Lyon, France.
4. Beland, F. A., and Kadlubar, F. F. (1990) in *Handbook of Experimental Pharmacology* (Cooper, C. S., and Grover, P. L., Eds.) Vol. 94/I, pp 267−325, Springer-Verlag, Heidelberg, Germany.
5. Kriek, E. (1992) *J. Cancer Res. Clin. Oncol. 118*, 481−489.
6. Heflich, R. H., and Neft, R. E. (1994) *Mutat. Res. 318*, 73−174.
7. Moriya, M., Takeshita, M., Johnson, F., Peden, K., Will, S., and Grollman, A. P. (1988) *Proc. Natl. Acad. Sci. U.S.A. 85*, 1586−1589.
8. Mah, M. C.-M., Boldt, J., Culp, S. J., Maher, V. M., and McCormick, J. J. (1991) *Proc. Natl. Acad. Sci. U.S.A. 88*, 10193−10197.
9. Carothers, A. M., Urlaub, G., Streigerwalt, R. W., Chasin, L. A., and Grunberger, D. (1986) *Proc. Natl. Acad. Sci. U.S.A. 83*, 9556−9560.
10. Carothers, A. M., Streigerwalt, R. W., Urlaub, G., Chasin, L. A., and Grunberger, D. (1989) *J. Mol. Biol. 208*, 417−428.

11. Shibutani, S., Suzuki, N., and Grollman, A. P. (1998) *Biochemistry 37*, 12034−12041.
12. Geacintov, N. E., Cosman, M., Hingerty, B. E., Amin, S., Broyde, S., and Patel, D. J. (1997) *Chem. Res. Toxicol. 10*, 111−146.
13. Patel, D. J., Mao, B., Gu, Z., Hingerty, B. E., Gorin, A., Basu, A. K., and Broyde, S. (1998) *Chem. Res. Toxicol. 11*, 391−407.
14. Singer, B., and Essigmann, J. M. (1991) *Carcinogenesis 12*, 949−955.
15. Cho, B. P., Beland, F. A., and Marques, M. M. (1994) *Biochemistry 33*, 1373−1384.
16. Eckel, L. M., and Krugh, T. R. (1994) *Biochemistry 33*, 13611−13624.
17. Mao, B., Gu, Z., Hingerty, B. E., Broyde, S., and Patel, D. J. (1998) *Biochemistry 37*, 81−94.
18. Mao, B., Gu, Z., Hingerty, B. E., Broyde, S., and Patel, D. J. (1998) *Biochemistry 37*, 95−106.
19. O'Handley, S. F., Sanford, D. G., Xu, R., Lester, C. C., Hingerty, B. E., Broyde, S., and Krugh, T. R. (1993) *Biochemistry 32*, 2481−2497.
20. Mao, B., Cosman, M., Hingerty, B. E., Broyde, S., and Patel, D. J. (1995) *Biochemistry 34*, 6226−6238.
21. Mao, B., Hingerty, B. E., Broyde, S., and Patel, D. J. (1995) *Biochemistry 34*, 16641−16653.
22. Mao, B., Gorin, A., Gu, Z., Hingerty, B. E., Broyde, S., and Patel, D. J. (1997) *Biochemistry 36*, 14479−14490.
23. Milhé, C., Dhalluin, C., Fuchs, R. P. P., and Lefèvre, J.-F. (1994) *Nucleic Acids Res. 22*, 4646−4652.
24. Milhé, C., Fuchs, R. P. P., and Lefèvre, J.-F. (1996) *Eur. J. Biochem. 235*, 120−127.
25. Cho, B. P., Beland, F. A., and Marques, M. M. (1992) *Biochemistry 31*, 9587−9602.
26. Mao, B., Vyas, R. R., Hingerty, B. E., Broyde, S., Basu, A. K., and Patel, D. J. (1996) *Biochemistry 35*, 12659−12670.
27. Melchoir, W. B., Jr., Matilde, M. M., and Beland, F. A. (1994) *Carcinogenesis 15*, 889−899.
28. Koffel-Schwartz, N., Verdier, J.-M., Bichara, M., Freund, A.-M., Daune, M. P., and Fuchs, R. P. P. (1984) *J. Mol. Biol. 177*, 33−51.
29. Bichara, M., and Fuchs, R. P. P. (1985) *J. Mol. Biol. 183*, 341−351.
30. Hoffman, G. R., and Fuchs, R. P. P. (1997) *Chem. Res. Toxicol. 10*, 347−359.
31. Zhou, L., Rajabjadeh, M., Traficante, D. D., and Cho, B. P. (1997) *J. Am. Chem. Soc. 119*, 5384−5389.
32. Sklenor, V., and Bax, A. J. (1987) *J. Magn. Reson. 74*, 469−479.
33. Bodenhausen, G., Gogler, H., and Ernest, R. R. (1984) *J. Magn. Reson. 58*, 370−388.
34. Friebolin, H. (1993) *Basic One- and Two-Dimensional NMR Spectroscopy*, 2nd ed., pp 263−291, VCH Publishers, New York.
35. Sandström, J. (1982) *Dynamic NMR Spectroscopy*, Academic Press, London.
36. Marky, L. A., and Breslauer, K. J. (1987) *Biopolymers 26*, 1601−1620.
37. Cramer, J. W., Miller, J. A., and Miller, E. C. (1960) *J. Biol. Chem. 235*, 885−888.
38. Kriek, E., Miller, J. A., Juhl, U., and Miller, E. C. (1967) *Biochemistry 6*, 177−182.
39. Shibutani, S., Gentles, R., Johnson, F., and Grollman, A. P. (1991) *Carcinogenesis 12*, 813−818.
40. Marques, M. M., and Beland, F. A. (1990) *Chem. Res. Toxicol. 3*, 559−565.
41. Arcos, J. C., and Argus, M. F. (1974) *Chemical Induction of Cancer*, Vol. IIB, Academic Press, New York.
42. Miller, E. C., Fletcher, T. L., Margreth, A., and Miller, J. A. (1962) *Cancer Res. 22*, 1002−1014.
43. Miller, J. A., Sandin, R. B., Miller, E. C., and Rusch, H. P. (1956) *Cancer Res. 15*, 188−199.
44. Fuchs, R. P. P., Lefevre, J.-F., Pouyet, J., and Daune, M. P. (1976) *Biochemistry 15*, 3347−3351.
45. Lefevre, J.-F., Fuchs, R. P. P., and Daune, M. P. (1978) *Biochemistry 17*, 2561−2567.
46. Iorio, M. A., Mazzeo-Farina, A., Seneca, L., and Boniforti, L. (1985) *Biol. Mass Spectrom. 12*, 30−37.
47. Nicoletti, M., and Iorio, M. A. (1986) *Magn. Reson. Chem. 24*, 221−224.
48. Evans, F. E., Miller, D. W., and Levine, R. A. (1983) *J. Am. Chem. Soc. 105*, 4863−4868.
49. Johnson, D. J., Reid, T. M., Lee, M.-S., King, C. M., and Romano, L. J. (1987) *Carcinogenesis 8*, 619−623.
50. Zhou, Y., and Romano, L. J. (1993) *Biochemistry 32*, 14043−14052.
51. Evans, F. E., Miller, D. W., and Levine, R. A. (1984) *J. Am. Chem. Soc. 106*, 396−401.
52. Stolarski, R., Hagberg, C.-E., and Shugar, D. (1984) *Eur. J. Biochem. 138*, 187−192.
53. Marques, M. M., Mourato, L. L. G., Santos, M. A., and Beland, F. A. (1996) *Chem. Res. Toxicol. 9*, 99−108.
54. Evans, F. E., and Levine, R. A. (1988) *Biochemistry 27*, 3046−3055.
55. Lasko, D. D., Basu, A. K., Kadlubar, F. F., Evans, F. E., Lay, J. O., and Essigman, J. M. (1987) *Biochemistry 26*, 3072−3081.
56. Shapiro, R., Sidawi, D., Miao, Y.-S., Hingerty, B. E., Schmidt, K. E., Moskowitz, J., and Broyde, S. (1994) *Chem. Res. Toxicol. 7*, 239−253.
57. Hansen, P. E., Dettman, H. D., and Sykes, B. D. (1985) *J. Magn. Reson. 62*, 487−496.
58. Lu, P., Metzler, W. J., Rastinejad, F., and Wasilewski, J. (1990) in *Structure and Function of Nucleic Acids and Proteins* (Wu, F. Y.-H., and Wu, C.-W., Eds.) pp 19−35, Raven Press, New York.
59. Rastinejad, F., Evilla, C., and Lu, P. (1995) *Methods Enzymol. 261*, 560−574.
60. O'Handley, S. F. (1991) Structural Analysis of a Carcinogen-Modified Oligomer by NMR Spectroscopy, Ph.D. Thesis, University of Rochester, Rochester, NY.
61. Roy, D., Hingerty, B. E., Shapiro, R., and Broyde, S. (1998) *Chem. Res. Toxicol. 11*, 1301−1311.
62. Shapiro, R., Ellis, S., Hingerty, B. E., and Broyde, S. (1998) *Chem. Res. Toxicol. 11*, 335−341.
63. Zhou, L., and Cho, B. P. (1998) *Chem. Res. Toxicol. 11*, 35−43.

BI990182D